

NMR Studies of the Stability, Protonation States, and Tautomerism of ^{13}C - and ^{15}N -Labeled Aldimines of the Coenzyme Pyridoxal 5'-Phosphate in Water[†]

Monique Chan-Huot,[‡] Shasad Sharif,[‡] Peter M. Tolstoy,[‡] Michael D. Toney,[§] and Hans-Heinrich Limbach^{*,‡}

[‡]*Institut für Chemie und Biochemie, Freie Universität Berlin, Takustrasse 3, D-14195 Berlin, Germany, and*

[§]*Department of Chemistry, University of California-Davis, Davis, California 95616, United States*

Received July 2, 2010; Revised Manuscript Received November 9, 2010

ABSTRACT: We have measured the pH-dependent ^1H , ^{13}C , and ^{15}N NMR spectra of pyridoxal 5'-phosphate ($^{13}\text{C}_2$ -PLP) mixed with equal amounts of either doubly ^{15}N -labeled diaminopropane, $^{15}\text{N}_\alpha$ -labeled L-lysine, or $^{15}\text{N}_\epsilon$ -labeled L-lysine as model systems for various intermediates of the transamination reaction in PLP-dependent enzymes. At low pH, only the hydrate and aldehyde forms of PLP and the free protonated diamines are present. Above pH 4, the formation of single- and double-headed aldimines (Schiff bases) with the added diamines is observed, and their ^{13}C and ^{15}N NMR parameters have been characterized. For 1:1 mixtures the single-headed aldimines dominate. In a similar way, the NMR parameters of the geminal diamine formed with diaminopropane at high pH are measured. However, no geminal diamine is formed with L-lysine. In contrast to the aldimine formed with the ϵ -amino group of lysine, the aldimine formed with the α -amino group is unstable at moderately high pH but dominates slightly below pH 10. By analyzing the NMR data, both the mole fractions of the different PLP species and up to 6 different protonation states including their pK_a values were obtained. Furthermore, the data show that all Schiff bases are subject to a proton tautomerism along the intramolecular OHN hydrogen bond, where the zwitterionic form is favored before deprotonation occurs at high pH. This observation, as well as the observation that around pH 7 the different PLP species are present in comparable amounts, sheds new light on the mechanism of the transamination reaction.

Vitamin B₆ or pyridoxal 5'-phosphate (**1**, PLP) is a cofactor of many enzymes responsible for a wide variety of amino acid transformations such as racemization, transamination, and decarboxylation among others. The different functional groups of PLP enable a surprisingly large number of chemical states, protonation states, and tautomeric states. In the active sites of enzymes, it forms a Schiff base generally termed the “internal aldimine” with the ϵ -group of a lysine residue (Scheme 1). When an amino acid substrate enters the active site, the internal aldimine is converted to an “external aldimine” (Scheme 1b) in which the α -amino group of the incoming amino acid forms the Schiff base (**1**). This transamination is common to all PLP-dependent enzymes and has been studied by a number of authors (2–10). It has been argued that the transamination requires a positive charge on the imino nitrogen of the Schiff base which is assisted by protonation of the pyridine ring. The latter should increase the equilibrium constant of the keto–enol tautomerism between an enolimine form and a ketoamine form as illustrated in Scheme 1a (11, 12). Indeed, a coupling between the two OHN hydrogen bonds has been confirmed recently by a combination of liquid- and solid-state ^{15}N NMR (13–18) of model Schiff bases. Also, microsolvation favors the ketoamine form (13). In this regard, alanine racemase represents a puzzle as X-ray studies suggest that the pyridine ring of the internal aldimine of PLP is not protonated (19). Therefore, microsolvation remains here the major explanation for the activation of PLP in alanine racemase,

as supported recently by theoretical calculations (20). The study of the tautomerism of PLP aldimines in water where microsolvation is maximized is, therefore, of special interest.

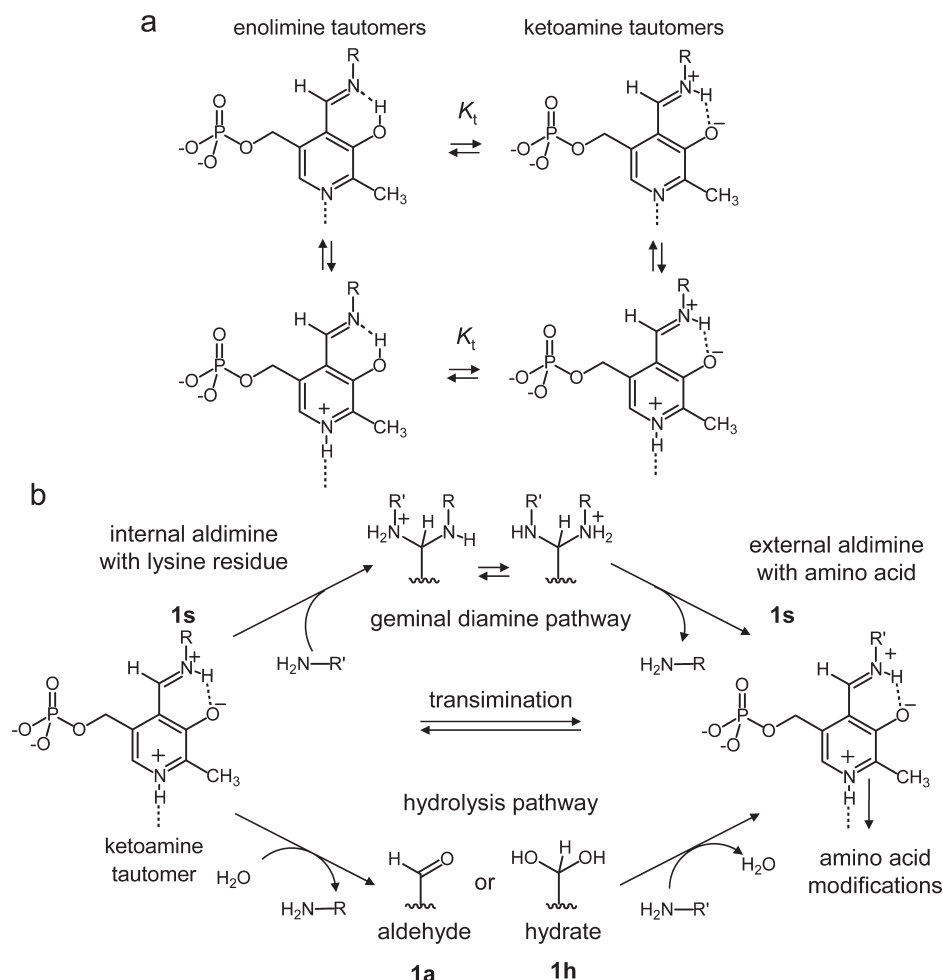
For the transamination reaction itself, two different hypotheses have been discussed. As illustrated in Scheme 1b, transamination could proceed via a geminal diamine formed by a direct addition of the amino group of the incoming amino acid to the internal aldimine. This pathway requires a base which accepts at least temporarily the proton of the ammonium group of the incoming amino acid. There are several reports in the literature which provide evidence for the geminal diamine pathway. An intermediate UV absorption around 340 nm was assigned to a singly protonated geminal diamine (5–7). Recently, a geminal diamine formed by an internal lysine and an external glutamate could be trapped and observed by X-ray crystallography (21), but its protonation states remained unknown; interestingly, the solid was found also to absorb light around 340 nm.

The transamination could also occur via the hydrolysis of the internal Schiff base involving a carbinolamine as intermediate (not shown) and the formation of the aldehyde or hydrate form of PLP, which are stabilized under acidic conditions (22). In a second step, the external aldimine may be formed with the substrate as illustrated in Scheme 1b (23, 24). This pathway involves a certain number of water molecules in the active site as well as stabilization of free PLP. To the present, it is not experimentally defined which pathway is realized and how it proceeds. However, it seemed to us that in order to obtain knowledge about the mechanism of the transamination the study of the interplay between chemical stability, protonation states, and tautomeric states under microsolvation with water molecules could be useful.

[†]This work has been supported by the Deutsche Forschungsgemeinschaft and the Fonds der Chemischen Industrie, Frankfurt.

*Corresponding author. Tel: +49 3083855375. Fax: +49 3083855310. E-mail: limbach@chemie.fu-berlin.de.

Scheme 1: (a) Keto–Enol Tautomerism between an Enolimine and a Ketoamine Form of Aldimines of Pyridoxal 5'-Phosphate (PLP, Vitamin B₆, **1**) in PLP-Dependent Enzymes.^a (b) Mechanisms of the Transimination Reaction Converting the Internal Aldimine to an External Aldimine with the Incoming Amino Acid Substrate.^b



^aProtonation of the pyridine ring (14) and an increase of the local solvent polarity (15) increase strongly the equilibrium constant of tautomerism K_t .^bThe transimination could proceed via a geminal diamine (upper pathway) or via hydrolysis with either the aldehyde or hydrate form of PLP as intermediate states. The nucleophilic attack of either an amino group or water is assisted by a positive charge of PLP in the ketoamine form.

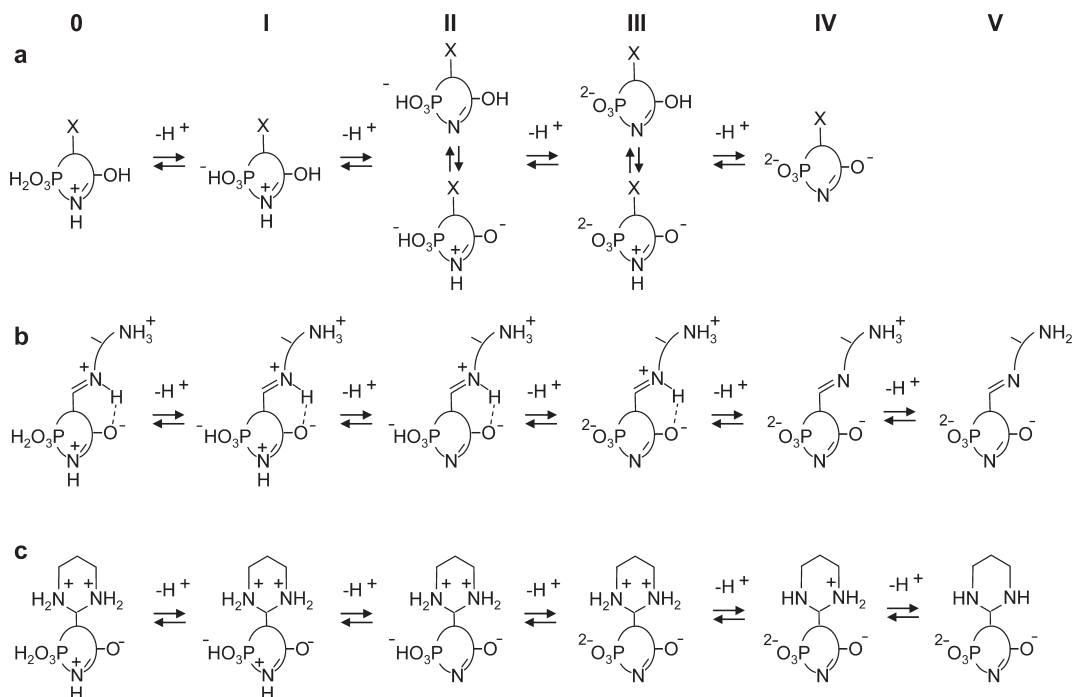
In the past, chemical and protonation states of PLP species have been often characterized using UV–vis absorption techniques (25–27). Also, enolimine and ketoamine forms give rise to different absorption bands (28). However, UV–vis spectroscopy lacks the chemical selectivity provided by multinuclear NMR spectroscopy, which was used in this study.

Until now, NMR studies of PLP species have focused on ¹H or ¹³C nuclei at natural abundance (23, 29, 30). Recently, some of us have used a combination of ¹³C and ¹⁵N NMR (18, 31) in order to establish the protonation states of isotopically labeled PLP. For PLP the reaction network of Scheme 2a could be established. In this scheme, for simplification, only the main functional groups are depicted. Five protonation states, 0–IV, were detected both for the aldehyde **1a** (X = CHO) and for the hydrate **1h** (X = CH(OH)₂), where II and III exhibited a tautomerism between the phenolic oxygen and the ring nitrogen. In principle, Schiff bases behave as illustrated in Scheme 2b for an arbitrary adduct of PLP with a diamine or an amino acid, but protonation states 0 and I are difficult to observe in aqueous solution as they decompose into **1a** and **1h** (28). ¹⁵N NMR parameters of the PLP Schiff base with methylamine in water were obtained recently (18). Schiff bases with diamines have attracted special attention (4) because they can form, in principle,

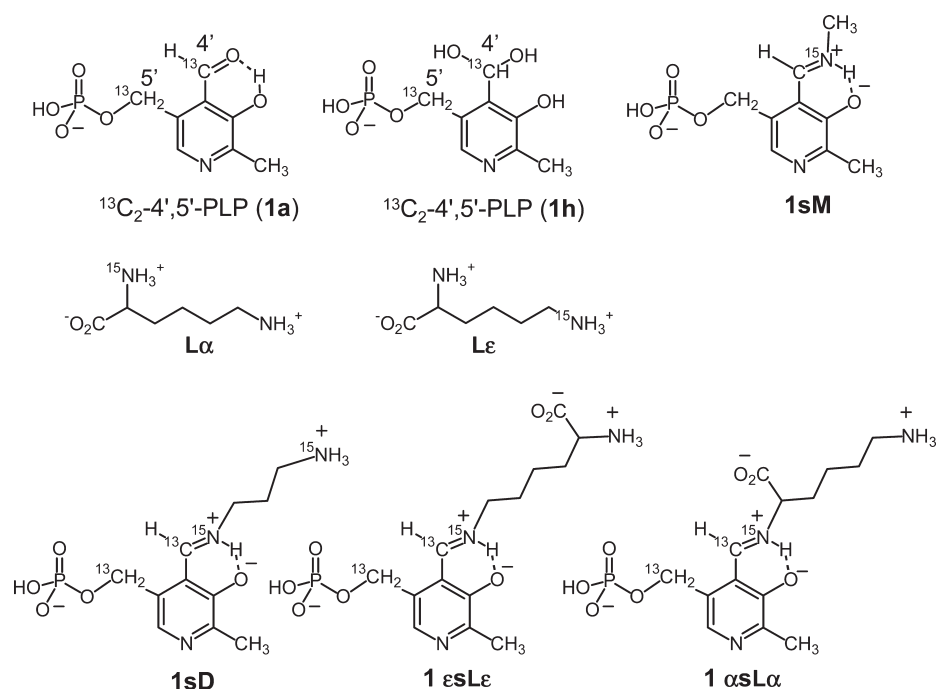
intramolecular cyclic geminal diamines. However, to date only diaminopropane **D** and some closely related compounds were found to form a geminal diamine **1gD**, a result which was attributed to the enhanced stability of six-membered rings (4, 28, 32). The protonation network one can expect for **1gD** is depicted in Scheme 2c.

The goal of this study is, therefore, to use multinuclear NMR to probe different chemical, tautomeric, and protonation states of PLP species and their relative thermodynamic stability in water where microsolvation is maximized. In particular, we wanted to explore ¹³C and ¹⁵N NMR as an effective tool. In order to exploit fully the possibilities of NMR, we synthesized PLP doubly labeled with ¹³C at C-4' and C-5' as depicted in Scheme 3. The synthesis of this compound, abbreviated as ¹³C₂-PLP, was performed (31) by a modification of the procedure of O'Leary et al. (33). We studied the following systems as models for species which might be involved in the transimination, i.e., the adducts with diaminopropane **D** as well as with L-lysine (**L**) as depicted in Scheme 3. The Schiff base **1sL** formed by PLP with the ε-amino group of **L** is a model for the internal aldimine, and the Schiff base **1asL** formed by PLP with the α-amino group of **L** is a model for the external aldimine. By labeling **D** doubly with ¹⁵N according to a procedure published previously (34), we could establish typical

Scheme 2: Protonation States of PLP Species: (a) Aldehyde Form **1a** and Hydrate Form **1h**; (b) Aldimine Form **1s** with an Amino Acid or Diamine; (c) Geminal Diamine **1g**



Scheme 3: Doubly ¹³C-Labeled PLP **1a** and **1h**, Single Schiff Base with ¹⁵N-Labeled Methylamine **1sM**, Single Schiff Base with Doubly ¹⁵N-Labeled Diaminopropane (**D**), and Single Schiff Bases **1sLε** and **1sLα** with Singly ¹⁵N- α -L-Lysine (**Lα**) and ¹⁵N- ϵ -L-Lysine (**Lε**)



¹³C and ¹⁵N chemical shift changes between the Schiff base **1sD** and the geminal diamine **1gD**. In the case of adducts of PLP with L-lysine, we found only two UV-vis studies of this system, one performed at pH 8.8 (35) and the other at pH 7.2 (36). A preliminary ¹H NMR study performed at pH 5.4, 6.8, and 11.6 gave evidence for the formation of the two Schiff bases (37). An ¹⁵N NMR study was only performed with L-lysine at natural abundance alone (38) and in the presence of formaldehyde (39). We chose to study commercially available L-lysine singly ¹⁵N-labeled

either in the ϵ -position (**Lε**) or in the α -position (**Lα**) as depicted in Scheme 3. This leads to the four Schiff bases, **1sLε**, **1sLα**, **1sLε**, and **1sLα**, of which two are illustrated in Scheme 3.

MATERIALS AND METHODS

Synthesis of ¹³C-Enriched PLP. ¹³C₂-PLP was synthesized as described previously (29).

Synthesis of ¹⁵N-Enriched Diaminopropane dihydrochloride. ¹⁵N₂-Diaminopropane dihydrochloride was prepared by using the

procedure of Scherer et al. (34). However, some modifications were introduced as described in the following.

¹⁵N₂-1,3-Diphthalimidopropane: Freshly distilled 1,3-dibromopropane (1.46 mL, 14 mmol, 1 equiv) was added to a solution of ¹⁵N-phthalimide (3.86 g, 26 mmol, 1.9 equiv) and dried with calcium carbonate (1.93 g, 14 mmol, 1 equiv) in dry DMF. Molecular sieve (4 Å) was added to the mixture before refluxing for 6 h. The reaction mixture was then stirred overnight at room temperature. After 50 mL of H₂O was added, a white precipitate was formed, and the reaction mixture was stirred for 1.5 h. The molecular sieves were removed. The precipitate was washed with methanol and ether. The solid was dissolved in dichloromethane, and the insoluble impurities were filtered off. After evaporation of dichloromethane with nitrogen, white crystals of ¹⁵N₂-1,3-diphthalimidopropane were obtained. Yield: 3.1 g, 71%, white crystal. *R_f* = 0.7 (benzene:acetic acid 9:1). ¹³C{¹H}-NMR (125 MHz, CD₂Cl₂): δ = 168.57 (s, C=O), 134.42 (d, aromatic), 132.54 (s, aromatic), 123.49 (d, aromatic), 36.16 (t, -N-CH₂-), 27.93 (t, -N-CH₂-CH₂-CH₂-N-). ¹H NMR (500 MHz, CD₂Cl₂): δ = 7.8 (m, 8H, aromatic), 3.7 (t, ³J(¹H, ¹H) = 7 Hz, 4H, CH₂ propane), 2.1 (quintuplet, 2H, CH₂ center, ³J(¹H, ¹H) = 7 Hz). MS (ESI-FT ICR MS): *m/z* = 695.1704 ([2 M + Na]⁺, *M*_{calc} = 695.1686), 375.0544 ([M + K]⁺, *M*_{calc} = 375.0531), 359.0808 ([M + Na]⁺, *M*_{calc} = 359.0792). IR (ZnSe diamond tip): ν = 3198, 1703, 1396, 1362, 1344, 1053, 1019, 893, 613 cm⁻¹.

¹⁵N-1,3-Diaminopropane dihydrochloride (D): Before the synthesis was started, ¹⁵N₂-1,3-diphthalimidopropane was recrystallized from CD₂Cl₂. Then, it was dissolved (1 g, 3 mmol, 1 equiv) in 4 mL of water containing calcium hydroxide (1.4 g, 24 mmol, 8 equiv). The solution was stirred for 3 days until it became clear at room temperature. The crude mixture was then subject to distillation until all liquid was removed, where the distillate was dropped into concentrated aqueous HCl solution. The dry residue was redissolved in 4 mL of water and subjected again to distillation, where the distillate was accumulated in the same flask as before. Redissolution of the dry residue and distillation were repeated five times. Finally, gaseous nitrogen was passed through the distillate in order to remove the solvent until white crystals of diaminopropane dihydrochloride appeared which were filtered and dried under high vacuum. Yield: 1.4 g, 68%, white crystal. *R_f* = 0.9 stained with ninhydrin (benzene:acetic acid 9:1), *R_f*(phthalic acid, side product) = 0.1. ¹³C{¹H}-NMR (125 MHz, D₂O): δ = 36.6 (t, NH₂-CH₂-), 24.8 (t, -CH₂-CH₂-CH₂-). ¹H NMR (500 MHz, D₂O): δ = 2.9 (t, 4H, ³J(¹H, ¹H) = 8 Hz, NH₂-CH₂-), 1.87 (quintuplet, 2H, ³J(¹H, ¹H) = 8 Hz, -CH₂-CH₂-CH₂-). MS (FAB (+), matrix H₂O/glycerol): *m/z* (%) = 77.1 ([M - 2Cl]⁺, 100). IR (ZnSe diamond tip): ν = 2937, 2175, 2093, 1609, 1544, 1475, 1365, 1185, 1051, 936, 751 cm⁻¹.

Sample Preparation. Aqueous solutions of 1:1 mixtures of PLP with diaminopropane or L-lysine with a final concentration of 120 mM were prepared prior to NMR measurements using water which was degassed and stored under argon in order to remove oxygen and carbon dioxide and prevent carbamate formation of the amines. One hour was given to reach equilibrium. The pH values of the solutions were adjusted before each spectroscopic measurement by addition of degassed 3, 1, or 0.1 M sodium hydroxide or hydrochloric acid solutions. A HANNA HI 9025 pH meter equipped with a HAMILTON Spinrode P electrode was used. The pH values were checked after the experiments and showed an average error of ±0.15.

For the UV-vis measurements we prepared a 1:1 solution of **1** and diaminopropane (**D**) exhibiting a final concentration of 0.1 mM.

Different samples were prepared depending on the experiment. For the ¹³C NMR experiments a solution of ¹³C₂-PLP with non-labeled diaminopropane was used. The ¹⁵N NMR experiments were performed with nonlabeled PLP and doubly ¹⁵N-labeled diaminopropane. ¹H and ¹³C NMR experiments were performed with ¹³C₂-PLP and ¹⁵N_ε L-lysine. The ¹⁵N NMR experiments were prepared with nonlabeled PLP mixed together with either ¹⁵N_α L-lysine or ¹⁵N_ε L-lysine. Both were purchased from Eurisotop and enriched at 95%. PLP was commercially available from Sigma Aldrich.

Spectroscopic Methods. All NMR measurements were performed at 278 K. UV-vis spectra were measured at 278 K on a PerkinElmer LAMBDA 25 spectrophotometer using a 1 cm quartz cuvette. NMR spectra were measured using a Bruker AMX 500 spectrometer (500.13 MHz for ¹H, 125.03 MHz for ¹³C, and 50.68 MHz for ¹⁵N). Inverse gated ¹H-decoupled ¹⁵N and ¹³C NMR spectra were recorded in H₂O with field locking on a D₂O-containing capillary with a recycle delay set to 10 s. The ¹⁵N spectra of neat nitromethane containing a D₂O capillary were recorded under the same ²H field locking conditions in order to reference the ¹⁵N chemical shifts. The relation δ(CH₃NO₂, liquid) = δ(¹⁵NH₄Cl, solid) - 341.168 ppm was used to convert the ¹⁵N chemical shifts from the nitromethane scale into the solid external ¹⁵NH₄Cl scale (40). For ¹³C NMR spectra, TMS was used as external reference.

RESULTS

In the following, we first describe the results of our pH-dependent NMR studies of mixtures of PLP with diaminopropane and then our NMR studies of L-lysine alone and in mixtures with PLP. All NMR experiments were performed at a concentration of 120 mM. The ¹H, ¹³C, and ¹⁵N NMR chemical shifts relevant to this study are assembled in Tables S1–S5 of the Supporting Information. pH-dependent UV-vis spectra were measured for a 1:1 mixture of diaminopropane (**D**) and of PLP (**1**) in water (0.1 mM, Figure S3 and Table S6 of the Supporting Information). The spectra were not analyzed in detail as it was difficult to distinguish protonation and tautomeric states of the different PLP species.

¹³C and ¹⁵N NMR of Mixtures of PLP with Diaminopropane in Water. Figure 1 depicts selected pH-dependent ¹³C and ¹⁵N NMR spectra of ¹³C₂-PLP in H₂O enriched to ~25% in positions C-4' and C-5' in the presence of an equimolar amount of doubly ¹⁵N-labeled diaminopropane (**D**). The chemical shifts depend slightly on pH, which is exploited below to characterize the protonation states of the different species. To facilitate the assignment, we have included the structures of the different species schematically at the top, using arbitrary but typical protonation states.

At low pH only the two ¹³C signals of the hydrate **1h** are observed, which are present also in the absence of **D** (31). Consequently, all ¹⁵N nuclei are localized in the free doubly protonated diamine **D**; they contribute a high-field signal around -8 ppm to the ¹⁵N spectrum. When pH is increased, the intensity of the hydrate signal decreases and new signals appear at lower field. At pH 6, a typical ¹³C-4' signal of the aldehyde **1a** can be identified around 195 ppm. This is in agreement with many previous observations that, on pH increase, the hydrate form of PLP is converted into the aldehyde (31, 22). This active form of PLP partially reacts with **D** to produce Schiff bases as indicated by the ¹³C-4' signals around 160 ppm. This signal does not exhibit a fine structure, and we assign it to a superposition of the single-headed Schiff base **1sD** and of the double-headed Schiff base **1dD**. The latter has been observed by ¹H NMR (28). However, in the

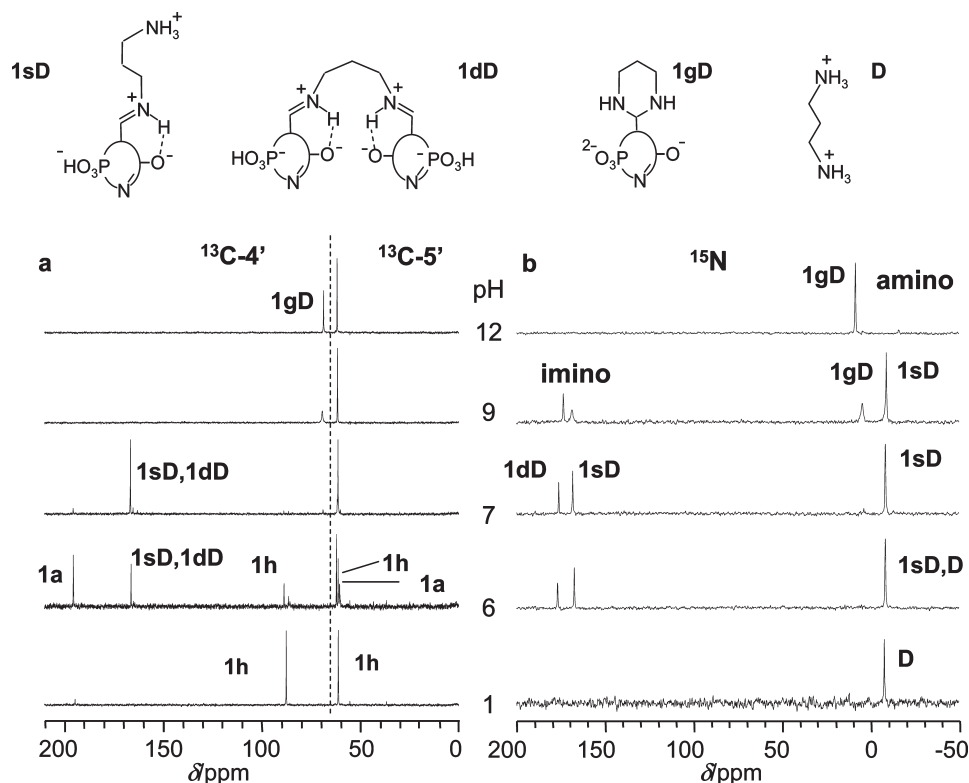


FIGURE 1: (a) Selected proton-decoupled ^{13}C and (b) ^{15}N NMR spectra of a 1:1 mixture of PLP and diaminopropane (**D**) in H_2O (120 mM) recorded at 278 K as a function of pH. Arbitrary protonation states are used in the chemical structures.

^{15}N NMR spectrum at pH 6 we observe two signals around 170 ppm, a value typical for Schiff bases. We assign the higher field signal to **1sD** and the lower field signal to **1dD**. The ^{15}N assignment is supported by experiments performed on the Schiff bases with L-lysine described in the next section. The -8 ppm signal in the ^{15}N spectrum at pH 6 corresponds to a superposition of the free amino groups of the single Schiff base **1sD** as well as of the free doubly protonated diamine **D**. In other words, it is difficult to distinguish between the free amino groups of **1sD** and **D** by ^{15}N NMR.

When pH is increased to 7, the aldehyde signal of **1a** disappears, as this species has been almost entirely converted to the imino signal of the Schiff bases. The ^{15}N signals do not change significantly. However, at pH 9, the ^{13}C -4' signal of the aldehyde has completely disappeared, and also the Schiff base signals are present only in traces. Instead, a broad signal around 68 ppm is observed, which we assign to the geminal diamine **1gD**. The latter has been observed previously by ^{13}C NMR (33). The corresponding ^{15}N signal of **1gD** appears at 4.73 ppm, exhibiting some line broadening. A similar line broadening is observed for the signal assigned to **1sD**.

We attribute the different amounts of **1sD** and **1dD** signals in the ^{13}C and ^{15}N spectra to small differences in pH. **1dD** has become less stable than **1sD**; the signal broadening of **1sD** and of **1gD** indicates an interconversion of both species in the second to millisecond time scale, whereas **1dD** interconverts more slowly. Finally, at very high pH, only the signals arising from the geminal diamine are observed by both ^{13}C and ^{15}N spectroscopy.

^{15}N , ^{13}C , and ^1H NMR Spectra of PLP in the Presence of L-Lysine. In this section, we describe the results of our multinuclear ^1H , ^{13}C , and ^{15}N NMR measurements on mixtures of isotopically labeled PLP and L-lysine. The chemical shifts again depend on pH, which is used below to characterize the protonation states of the species observed.

In the first stage, we measured the ^{15}N NMR spectra of $^{15}\text{N}_\epsilon$ L-lysine (**Le**) and of $^{15}\text{N}_\alpha$ L-lysine (**La**) as a function of pH. Spectra and chemical shifts (included in the Supporting Information) are used below to determine the pK_a values and the limiting ^{15}N chemical shifts of the different protonations states. These data were useful for detecting chemical shift differences between the free ammonium groups in the adducts with PLP. In Figure 2a, the pH-dependent ^{15}N spectra of a sample containing a 1:1 mixture of PLP with $^{15}\text{N}_\epsilon$ L-lysine (**Le**) and in Figure 2b a similar mixture with $^{15}\text{N}_\alpha$ L-lysine (**La**) are depicted. At the top, the proposed chemical structures are included, drawn in arbitrary protonation states. At low pH, only the signals of the free amino groups are observed at -8 and -1 ppm, as corroborated by the corresponding spectra in the absence of PLP (see Supporting Information and ref 39). When the pH is increased to 5, new signals appear around 150 ppm, corresponding to the Schiff bases formed with both the ϵ - and α -amino groups of lysine. The chemical shift represents an average of both the enolimine and the ketoamine shifts and will be analyzed later. Two signals are observed: the low-field lines correspond to the double-headed Schiff bases and the high-field lines to the single-headed Schiff bases, as demonstrated by the expanded signals at pH 8 in Figure 2. This assignment was corroborated by increasing the amount of PLP, which increases the low-field signals (see Supporting Information). The different chemical shifts of the two species reflect a different equilibrium constant for the enolimine–ketoamine tautomerism.

When pH is further increased, the nitrogen imino signals broaden substantially. **1asLa** is hydrolyzed at pH 13, and the ^{15}N label reappears as free L-lysine. By contrast, **1esLe** is not hydrolyzed and reappears at low field around 300 ppm, which is typical for deprotonated Schiff bases. No signal for a geminal diamine can be detected.

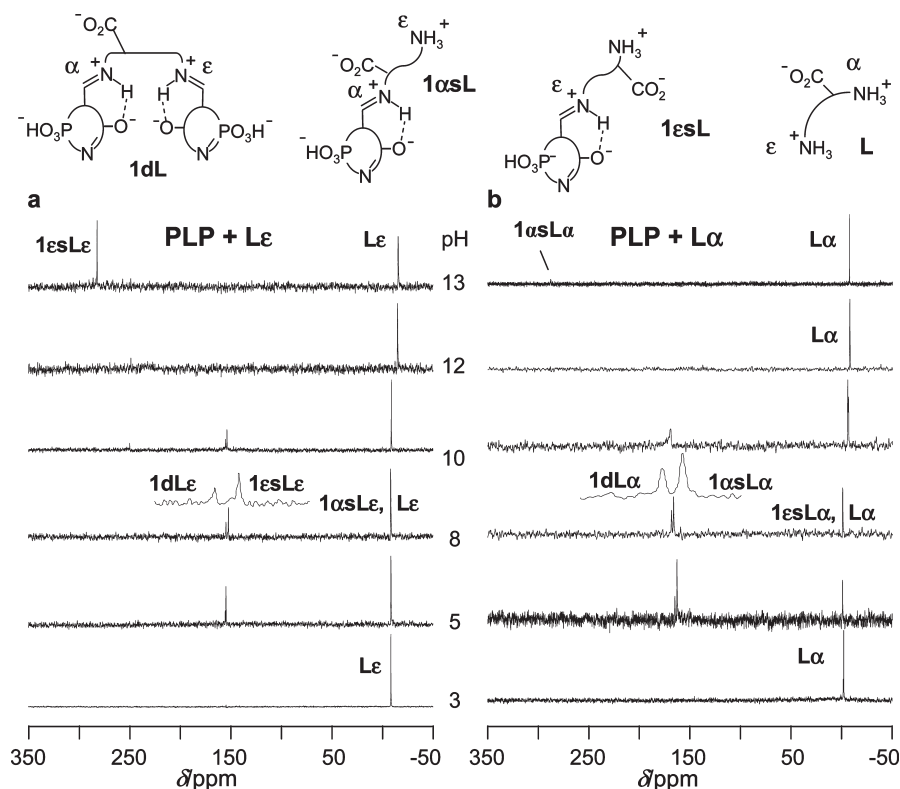


FIGURE 2: Selected proton-decoupled ^{15}N NMR spectra of 1:1 mixtures (120 mM) of $^{13}\text{C}_2$ -PLP with (Le) (a) and (La) (b) at 278 K using H_2O as solvent. Arbitrary protonation states are used in the chemical structures. The inserted signals at pH 8 were expanded by a factor of 4.

The ^{15}N NMR studies provide a general view on the interaction of the PLP with L-lysine, in particular the absence of a geminal diamine, the hydrolysis of the Schiff base $1\alpha\text{SL}\alpha$, and the stability of $1\epsilon\text{SL}$ at high pH. However, it is difficult to obtain information about the equilibrium between $1\epsilon\text{SL}$ and $1\alpha\text{SL}\alpha$ by ^{15}N NMR. Therefore, we performed ^{13}C NMR measurements of $^{13}\text{C}_2$ -PLP in the presence of an equimolar amount of Le at different pH values. In Figure 3a selected spectra of a 1:1 mixture of PLP and Le in H_2O are depicted. Again, no signal for a geminal diamine is observed at high pH, which would be expected around 70 ppm. Whereas the ^{13}C -5' signal is of little diagnostic value, the ^{13}C -4' signals exhibit major changes with pH. At pH 3, as expected, the hydrate form 1h of free PLP dominates, and to a smaller extent the aldehyde 1a is observed. Schiff bases are present only in trace amounts. However, when pH is increased, 1h disappears and Schiff base signals appear around 166 ppm. At pH 13, the aldehyde 1a reappears when $1\alpha\text{SL}$ is hydrolyzed, and only the signal of the imine carbon of $1\epsilon\text{SL}$ remains.

The assignment of the Schiff base signals was done by analyzing their ^{13}C - ^{15}N coupling patterns. As a demonstration, we have included in Figure 3a expanded signals obtained with D_2O as solvent at pH 10, where all ^1H - ^{13}C couplings are removed. This spectrum contains four signals. Only the two low-field signals exhibit a coupling $^1J(^{13}\text{C}, ^{15}\text{N}) = 19$ Hz whereas the two signals at high field are singlets. By ^{15}N NMR we know that the single-headed Schiff base dominates for 1:1 mixtures of PLP with L-lysine. These observations allow us to assign the signals and obtain their chemical shifts as illustrated in Figure 3a. This analysis also indicates that the equilibrium $1\alpha\text{SL} \leftrightarrow 1\epsilon\text{SL}$ is shifted below pH 10 to the left and above pH 12 to the right side.

Finally, we have performed ^1H NMR measurement of 1:1 mixtures of $^{13}\text{C}_2$ -PLP with Le in order to obtain the relative mole fractions of all species as a function of pH. All H-4' proton signals

are split into doublets by ^1H - ^{13}C scalar coupling with the corresponding enriched ^{13}C -4' nuclei of PLP. The aldehyde and Schiff base signal regions are depicted in Figure 3b. Within the resolution of our experiments, no scalar coupling from ^1H or ^{13}C to the ^{15}N nucleus of the lysine residue was observed. The signal assignment for Figure 3b was straightforward, taking into account the results obtained by ^{15}N and ^{13}C NMR. It was confirmed that $1\alpha\text{SL}$ dominates slightly over $1\epsilon\text{SL}$ below pH 10 whereas the reverse is true above pH 12.

Chemical Shifts and pK_a Values. Generally, average chemical shifts of species subject to different protonation states can be expressed as a function of pH using the Henderson–Hasselbalch equation (41, 42) adapted for NMR spectroscopic methods in the fast proton exchange regime (43). For free PLP in the aldehyde form 1a and the hydrate form 1h recently five different protonation states were identified as illustrated in Scheme 2a (18, 31). For the single-headed Schiff bases with primary amines, one can formulate five protonation states, whereas six states are conceivable for Schiff bases with diamines or with L-lysine (Scheme 2b). The Henderson–Hasselbalch equation for six protonation states can be written in the form

$$\delta_{\text{obs}} = \delta_0 + \sum_i (\delta_{i+1} - \delta_i) \frac{10^{\text{pH} - \text{p}K_{a_i}}}{1 + 10^{\text{pH} - \text{p}K_{a_i}}}, \quad i = 0 - \text{IV} \quad (1)$$

As usual, $\text{p}K_{a_i}$ represents the pH values where protonation states i and $i + 1$ exhibit the same concentration. δ_i represents the limiting chemical shift of protonation state i . Equation 1 is valid for all nuclei of PLP.

The ^{15}N chemical shifts of the single Schiff base 1SD , of the geminal diamine 1GD , and of the double Schiff base 1DD formed in mixtures of PLP with diaminopropane D are plotted in Figure 4 as a function of pH. For comparison, we have added in Figure 4a

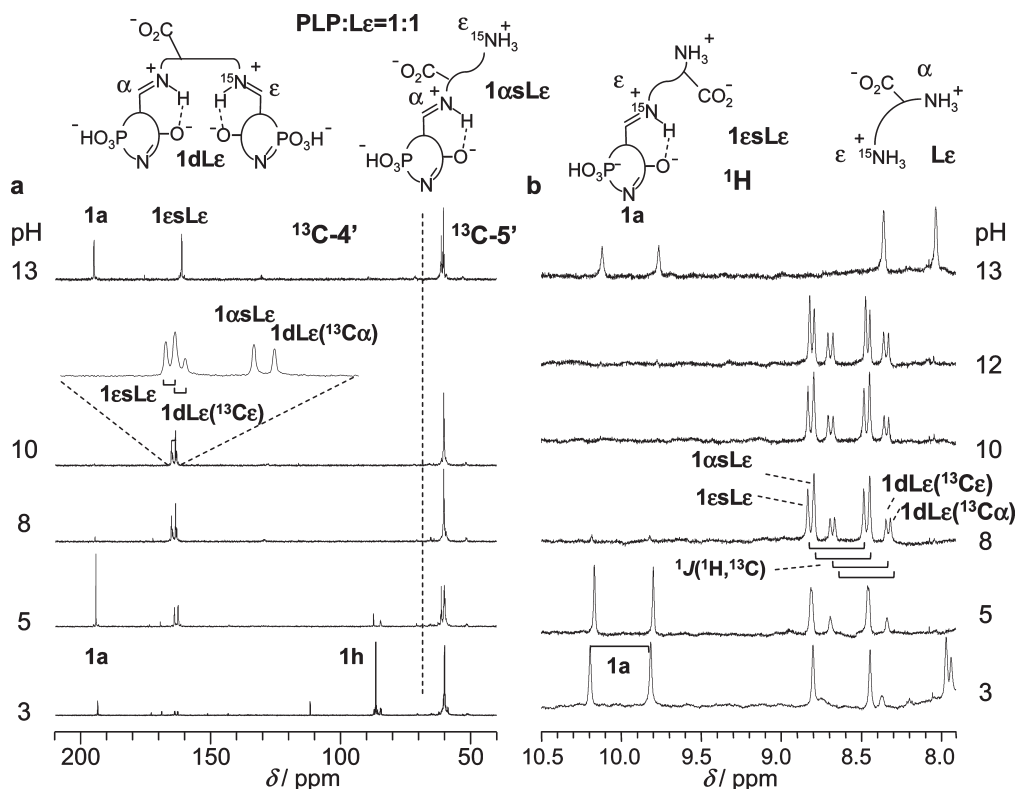


FIGURE 3: (a) ^{13}C NMR spectra and (b) ^1H NMR spectra of equimolar mixtures (120 mM) of $^{13}\text{C}_2$ -PLP and L in H_2O at 278 K. The expanded ^{13}C spectrum at pH 10 was obtained using D_2O . Arbitrary protonation states are used in the chemical structures.

the ^{15}N chemical shifts measured previously (18) of the PLP-methylamine Schiff base **1sM** labeled in the imino position (lower dashed curve) and in the pyridine ring (upper dashed curve). In order to simulate the data, we assumed that the ^{15}N chemical shifts δ_0 and δ_{IV} of protonation states 0 and IV in eq 1 at low and high pH are similar to those measured previously for methylamine PLP and other Schiff bases (18, 44). The solid lines were calculated by fitting the calculated data points to the experimental ones using eq 1, without variation of δ_0 and δ_{IV} , but optimizing the chemical shifts δ_{I} , δ_{II} , and δ_{III} of the remaining protonation states and the corresponding pK_a values. The latter are marked in Figure 4 as vertical dashed lines separating the different protonation states. All parameters obtained are assembled in Table 1. Note that protonation states I–III are subject to enolimine–ketoamine tautomerism and that the values of δ_{I} , δ_{II} , and δ_{III} in eq 1 provide information about the equilibrium constant K_{I} of the tautomerism as shown later. Note also that the upper dashed line representing the ^{15}N chemical shifts of the pyridine ring of **1sM** indicates deprotonation of the latter at pH 5.8.

Finally, Henderson–Hasselbalch plots of the ^{15}N NMR chemical shifts of the Schiff base nitrogens of PLP with the L-lysines **1a** and **1e** enriched at the α - and at the ϵ -position are shown in Figure 5. The solid lines were calculated using a fixed value of δ_0 taken from the data of the PLP-methylamine Schiff base **1sM** (dashed curves). δ_{I} , δ_{II} , δ_{III} , and δ_{IV} were obtained by fitting the data to eq 1. Unfortunately, as illustrated in Figure 5a, we had only a single ^{15}N NMR chemical shift value at high pH in order to determine δ_{IV} . This value was then fixed and used in order to calculate the solid curve in Figure 5b. As the ^{15}N chemical shifts of the Schiff base nitrogen atoms are not sensitive to the protonation states of the free ammonium groups, their pK_a values were taken from those of free L-lysine and were not varied in the fitting pro-

cedure, in contrast to the remaining pK_a values. All data describing the solid lines in Figure 5 are included in Table 1. For comparison, we added data obtained previously by ^{15}N NMR and by colorimetry.

We cannot detect a substantial difference between the single- and double-headed Schiff bases, with the exception that their mole fractions at high pH are too small to be observed.

Determination of the Mole Fractions of Different PLP Species. In the case of the 1:1 mixture of PLP with diaminopropane, the mole fractions x_{1a} and x_{1h} of **1a** and **1h** of the free PLP species are calculated from the integrated ^{13}C -4' signal intensities of the different species. Since the ^{13}C -4' signals of the single- and the double-headed Schiff bases **1sD** and **1dD** were not resolved, only the sum of their mole fractions could be determined. However, these values could be obtained from the corresponding ^{15}N signal intensities. The results are included in the Supporting Information, and plots of the mole fractions against the pH are shown in Figure 6a.

At very low pH, doubly protonated free diaminopropane **D** and the hydrate **1h** predominate. From pH 4, the mole fraction of the aldehyde **1a** increases as does the formation of the single-headed Schiff base **1sD**. In neutral solution, the hydrate **1h** is completely converted into the aldehyde form of PLP **1a**, which reacts with diaminopropane **D** to form more Schiff bases. The single-headed Schiff base **1sD** predominates up to pH 9. At very high pH, only the geminal diamine **1gD** is present in the solution.

The mole fractions of the PLP species reacting with L-lysine were obtained from the integrated signal intensities of the H-4' NMR signals (Figure 3). The results are given in Table 1 and are plotted in Figure 6b as a function of pH. In acidic solution, the hydrate form of PLP **1h** is the dominant species. As pH is increased, the hydrate form of PLP **1h** converts into the active

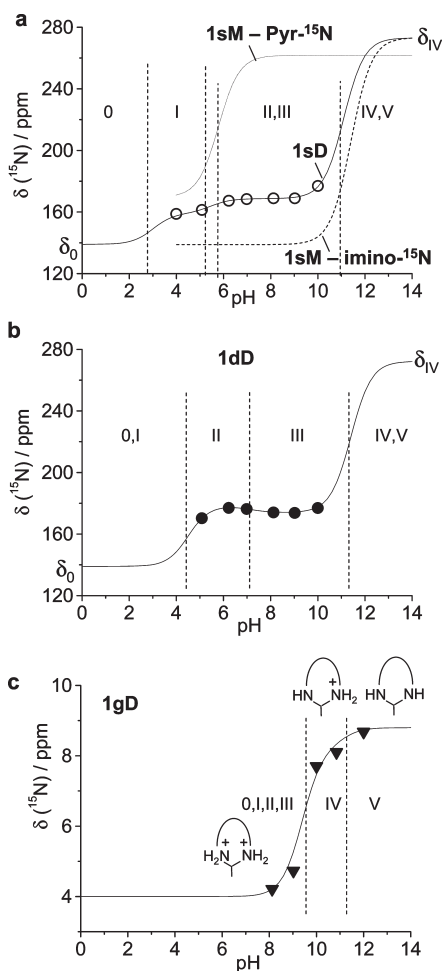


FIGURE 4: (a) Henderson–Hasselbalch plot of the ^{15}N chemical shifts of the single PLP Schiff base with diaminopropane **1sD**. For comparison we have added the corresponding data (dashed curves) of the PLP methylamine Schiff base **1sM** studied in ref 18 (concentration 40 mM). (b) Corresponding plot of the double-headed Schiff base **1dD** and (c) of the geminal diamine **1gD**. The solid lines were fitted to the experimental data using the Henderson–Hasselbalch equation as described in the text, without variation of the limiting values δ_0 and δ_{IV} taken from **1sM**. The dashed vertical lines mark the calculated pK_a values. The protonation states are labeled with roman numbers according to Scheme 2.

aldehyde **1a** which forms Schiff bases **1esL** and **1asL** in equal amounts. This balance is perturbed above pH 6, where the mole fraction of **1esL** becomes larger than that of **1asL**. This situation remains constant until very high pH 12 where **1asL** is hydrolyzed into **1a** and **L**, whereas **1esL** remains stable.

DISCUSSION

pH Dependence of PLP Species and Their Protonation States. Figure 7 provides an overview of the different PLP species and their reaction partners as a function of pH. The intensity of the vertical bars indicates schematically the relative mole fraction of a given species. The protonation states of Scheme 2 are represented by roman numbers. pK_a values that have been determined are represented by horizontal lines inside the vertical bars separating the protonation states. In order to facilitate the discussion, we include schematic chemical formulas illustrating the protonation state exhibiting the highest probability in the whole pH range. The PLP species formed by reaction with diaminopropane are depicted on the left side of Figure 7 and on the right side those by reaction with L-lysine.

Below pH 4, only free, doubly protonated L-lysine (**L**) or diaminopropane (**D**) are present in a mixture with PLP, for which the hydrate form **1h** dominates as expected from previous studies (18, 31). The formation of single-headed and double-headed Schiff bases starts above pH 4. L-Lysine can form two different single-headed Schiff bases with PLP, either **1esL**, involving the ϵ -amino group, or **1asL**, involving the α -amino group. Whereas **1esL** remains stable when pH is increased and predominates at high pH values, surprisingly, **1asL** hydrolyzes at pH 12. The single-headed Schiff base **1sD** with diaminopropane shows a different behavior; above pH 8 it is converted into a geminal diamine species **1gD** which becomes the only product at very high pH. This species is clearly deprotonated on the amino nitrogen atoms; it shows characteristic ^{15}N and ^{13}C NMR chemical shifts (Supporting Information Table S1). Interestingly, we observed an UV absorption band at 310 nm (Supporting Information Figure S3). This value is smaller than the value of about 340 nm reported previously for geminal diamine intermediates of PLP-dependent enzyme reactions (5–7, 21). One can then conclude that the latter value corresponds to singly, probably doubly protonated geminal diamine species and that the latter is unstable in water.

It follows that the free energies of the different species are controlled by protonation/deprotonation processes, but how is this feature related to the acid–base properties of the individual functional groups? A look at Figure 7 indicates that the acid–base properties of the pyridine ring play the most important role. The Schiff bases start to lose the pyridinium proton at pH 4 when protonation state I is converted to II. By contrast, as described previously (18, 31), protonation state II of **1a** and **1h** is characterized by a fast tautomerism of the proton between the pyridine nitrogen and the phenolic oxygen. Nevertheless, deprotonation of the pyridine ring is the starting point for the formation of the Schiff bases as illustrated by the dashed horizontal line at pH 4. However, the Schiff bases become dominant only when **1h** and **1a** lose the pyridinium proton as well as the remaining phosphate proton in protonation state III. We find only minor differences of the occurrence of the single- and the double-headed Schiff bases, indicating that the two amino groups of diaminopropane and L-lysine react independently of each other.

As far as the stability of the geminal diamine is concerned, it is plausible that it is destroyed by single or double protonation as illustrated in Scheme 2c. Probably, solvation of the resulting ammonium groups plays here an important role. Metzler et al. (28, 32) showed that only diaminopropane forms geminal diamines with PLP but not other diamines, a circumstance which they attributed to the stability of 6-membered rings. Our attempts to observe a geminal diamine with L-lysine at high pH were unsuccessful. Only **1esL** remains, entirely deprotonated in state V, but does not show any tendency to form a geminal diamine.

One remarkable conclusion can be drawn from the overview of Figure 7. There is one pH where almost all PLP species (free aldehyde, hydrated PLP, and single Schiff bases) are present in a comparable amount, which is approximately pH 7. We discuss the implications of this finding below.

Tautomerism of PLP Schiff Bases in Water. We come now to the question of the proton tautomerism of Schiff bases involving the intramolecular OHN hydrogen bonds depicted in Scheme 1a. The question is whether or not we can obtain information about this process with water as solvent. Previously, in the case of the PLP-methylamine Schiff base (18) only the

Table 1: ^{15}N Chemical Chemical Shifts δ and pK_a Values of PLP, Diaminopropane, Lysine and Corresponding PLP Species^a

	reference	method	δ_0	δ_{I}	δ_{II}	δ_{III}	δ_{IV}	δ_{V}	pK_{a0}	pK_{a1}	pK_{a2}	pK_{a3}	pK_{a4}
PLP + alanine	28	colorimetry							3.02	5.44	6.57	11.78	
										5.38	6.89	11.97	
											6.01	11.86	
PLP + methylamine	18	^{15}N NMR		264.0	170.4		272.3	139.0		5.8		11.4	
1sD	Figure 4	^{15}N NMR	139.0 ^b	159	168.7		272.3 ^b		3.0	5.4		11.1	
1αsL	Figure 5	^{15}N NMR	139.0 ^b		163	167.3	305			4.0	6.4	11.4	
1ϵsL	Figure 5	^{15}N NMR	139.0 ^b		155	151	286			4.0	6.8	11.4	
1dD	Figure 4	^{15}N NMR	139.0 ^b	178.4	173.9	272.3 ^b				4.5	7.1	11.4	
1dLα	Figure 5	^{15}N NMR	139.0 ^b	164	168.3	305				4.0	6.4	11.4	
1dLϵ	Figure 5	^{15}N NMR	139.0 ^b	155	151.6	286				4.0	6.8	11.4	
1gD	28	colorimetry								5.55		9.14	11.08
										5.35			
1gD	Figure 4	^{15}N NMR				4.0	8.3	8.7		n.o.		9.4	11.1
L	38	colorimetry							2.2	9.1	10.5		
Lα	39	^{15}N NMR	-0.6	0.4	-6.1	-7.6							
Lϵ	39	^{15}N NMR	-6.2	-7.1	-9.2	-15.2			2.2	9.6	11.5		
Lα	Supporting Information	^{15}N NMR	-2.39	-0.19	-3.69	-7.31			2.2	9.0	10.0		
Lϵ	Supporting Information	^{15}N NMR	-7.00	-7.20	-8.00	-15.65			2.2	8.8	10.8		
D	28	colorimetry										9.01	10.4

^a ^{15}N chemical chemical shifts δ in ppm with respect to solid $^{15}\text{NH}_4\text{Cl}$. ^b Limiting chemical shifts taken from PLP methyl Schiff base from Sharif et al. (18) n.o.: not observed.

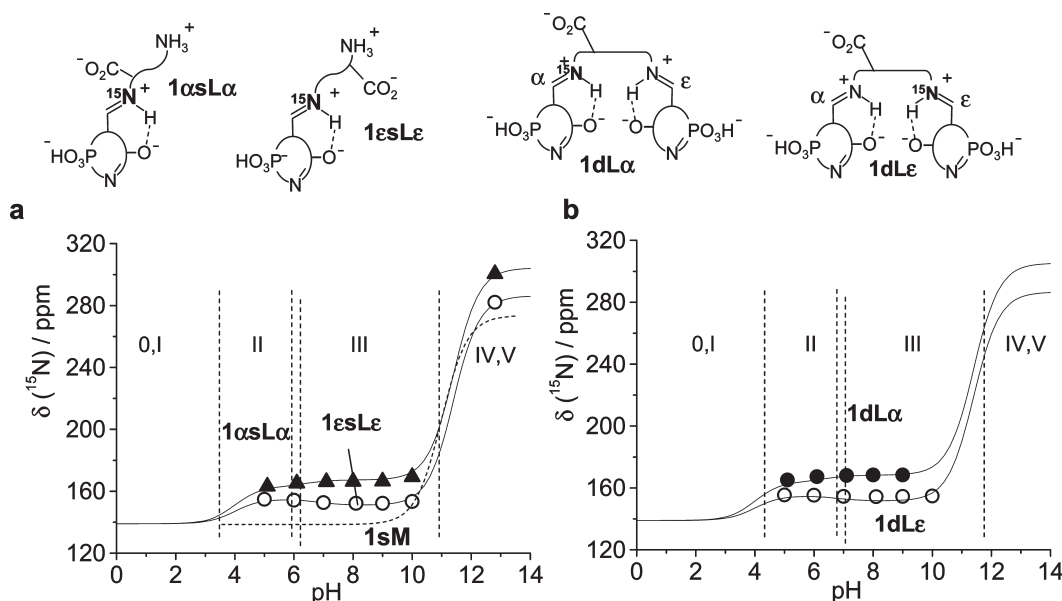


FIGURE 5: (a) Henderson–Hasselbalch plot of the ^{15}N chemical shifts of the single-headed Schiff bases **1 α sL α** and **1 ϵ sL ϵ** . For comparison we have added the corresponding data (dashed curve) of the PLP-methylamine Schiff base **1sM** studied in ref 18. (b) Corresponding plot of the double-headed Schiff bases **1dL α** and **1dL ϵ** . Arbitrary protonation states are used in the chemical structures. For further description see legend of Figure 7.

zwitterionic form was observed, giving rise to a ^{15}N chemical shift of 139 ppm. At high pH, the proton is lost, leading to a strong low-field shift. This behavior was illustrated in Figure 4a and in Figure 5a as dashed curves. It was discussed in terms of the possibility that the intramolecular OHN hydrogen bond is destroyed by interaction with water (18). The ^{15}N chemical shifts of the Schiff bases of PLP with diaminopropane and L-lysine were, therefore, a surprise; the limiting ^{15}N chemical shift of 139 ppm for the zwitterionic form was not achieved above pH 4 where the Schiff bases are observed. Clearly, as has been discussed previously for other environments (13–15, 23), this observation is evidence that the tautomerism, and hence the intramolecular OHN hydrogen bond, is intact in water.

Estimates of the equilibrium constants K_t of tautomerism can be obtained from the equation

$$K_t = \frac{\delta_{\text{N}} - \delta_{\text{obs}}}{\delta_{\text{obs}} - \delta_{\text{NH}}} \quad (2)$$

where δ_{obs} is the observed ^{15}N chemical shift of a given Schiff base at a given pH, $\delta_{\text{NH}} = 139$ ppm is the limiting chemical shift of the NH form, taken from the PLP-methylamine Schiff bases, and $\delta_{\text{N}} = 255$ ppm the limiting chemical shift of the OH form, where the proton is hydrogen bonded to nitrogen. Complete removal of the proton would increase this value up to 290 ppm as found in the case of **1 ϵ sL ϵ** at high pH (Figure 5a). Using the

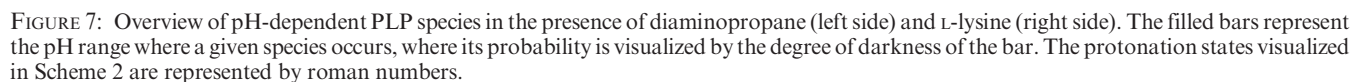
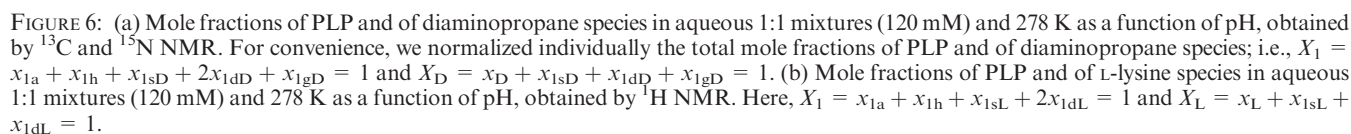


Table 2: Equilibrium Constants K_t of the OHN Tautomerism of PLP Schiff Bases

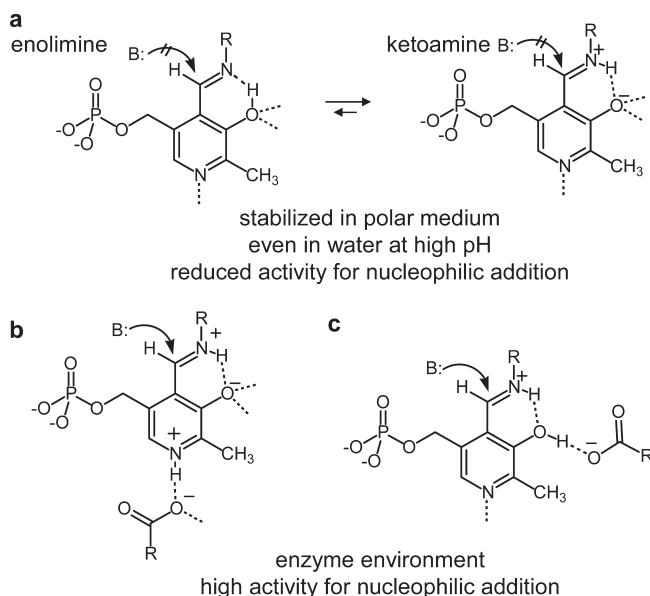
pH	1sD	1dD	1εsLε	1dLε	1αsLα	1dLα
4	4.9					
5	4.2	2.7	6.3	6.0	3.8	3.4
6	3.1	2.0	6.6	6.1	3.4	3.1
7	2.9	2.1	7.4	6.5	3.3	3.0
8	2.9	2.3	7.8	6.5	3.2	2.9
9	2.9	2.3	7.8	6.5	3.2	2.9
10	2.0		7.0	6.3	2.8	

^{15}N chemical shifts assembled in the Supporting Information, and neglecting a potential influence of the solvent on the limiting chemical shifts, we estimate using eq 2 the equilibrium constants K_t assembled in Table 2. All equilibrium constants K_t are larger than unity, favoring the zwitterionic forms. This effect arises from the high solvent polarity, which was identified previously as one of the factors favoring the zwitterionic forms (13–15). At low pH, the values of K_t increase slightly due to protonation of the pyridine ring, which is another factor leading to dominance of the zwitterionic forms (13–15). Between pH 4 and 10 the values remain fairly constant. Above pH 10, deprotonation of the intramolecular OHN hydrogen bond occurs. No significant difference is observed for the single- and the double-headed Schiff bases. The values of K_t for the Schiff bases with diaminopropane and with the α -amino group of L-lysine are very similar. In contrast, those for the Schiff bases with the ϵ -amino groups are substantially larger, as expected for the higher basicity of this nitrogen atom.

Implications for the Biological Function of PLP. Let us discuss now whether the properties of PLP and its Schiff bases elucidated here by multinuclear NMR have any implications for the biological function of PLP. In particular, what can one conclude about the transamination reaction pathway depicted in Scheme 1b? This study was performed in aqueous solution, where the solvent polarity will be larger than in the active sites of PLP-dependent enzymes (16). Moreover, aqueous solution provides the limiting case of maximal solvent polarity achieved either by water in the active site or by polar groups of amino acid side chains.

As discussed above, Figure 7 indicates that at physiological pH, all important PLP species (the aldehyde, the hydrate, and the two Schiff bases of PLP with L-lysine) are present in aqueous solution, although the Schiff bases dominate. pH alteration changes the equilibrium of the formation of the aldimines from free PLP to a much greater extent than changes in the total concentrations of the 1:1 mixtures; our present NMR studies were performed at 120 mM and the UV–vis studies (Supporting Information) at 0.1 mM, and in our previous study of the methylamine Schiff base (18) we employed a concentration of 40 mM. Qualitatively, we obtained in all cases comparable mole fractions of the different PLP species around pH 7. Naturally, the situation might be modified in the active site of PLP-dependent enzymes. The observed thermodynamic equivalence of free PLP and PLP in the aldimine form at pH 7 indicates that none of these species constitute a high-energy intermediate that could provide a bottleneck for the hydrolysis pathway of the transamination (Scheme 1b). Only the geminal diamine is unfavorable at pH 7, since the attacking amino groups have to be deprotonated prior to the nucleophilic addition. These findings favor hydrolysis as the pathway for transamination.

Scheme 4: (a) Stabilization of the Ketoamino Forms of PLP Schiff Bases in a Polar Environment by Microsolvation, e.g., in Water up to pH 10.^a (b) Activation of PLP Schiff Bases for Nucleophilic Addition by Creating a Positive Charge by Protonation and Hydrogen Bonding of the Pyridine Ring As Found for Aspartate Aminotransferase (16). (c) Possible Activation by Protonation of the Phenolic Oxygen As Suggested by the Crystal Structure of Alanine Racemase (19)



^aThe ketoamine does not exhibit a net positive charge.

On the other hand, in general it is found that mutant PLP enzymes, in which the Schiff base-forming lysine is mutated, bind amino acids much tighter than do the corresponding wild-type enzymes. With AAT for example, the K258A mutant binds aspartate $\sim 10^5$ -fold tighter (45). This was hypothesized to be due to the removal of the ϵ -amino group of K258, which competes with the substrate amino group for Schiff base formation in the Michaelis complex. One could then conclude that the equilibrium constant for Schiff base formation between K258 and PLP is $\sim 10^5$ in the Michaelis complex and that hydrolysis is unfavorable. This would suggest that the external aldimine is formed through a geminal diamine intermediate as supported by several authors (5–7, 21). However, as discussed above, according to the difference of the UV spectra of these intermediates and those of 1gD at high pH, the geminal intermediates are singly or doubly protonated, i.e., in a state which is not stable in water. An unsolved interesting question is then how the enzyme stabilizes such a state.

On the other hand, the present results add to our understanding of the activation of the internal aldimine in the active sites of PLP-dependent enzymes. As illustrated in Scheme 4a, even when the pyridine ring is not protonated under neutral conditions, the tautomerism of aldimines in a polar environment is shifted toward the zwitterionic ketoamine form, but some of the enolimine form is still present. Both forms are found to be in slow exchange within the NMR time scale with remaining free PLP. By contrast, the zwitterionic ketoamine form is favored strongly when the pyridine ring becomes protonated. Thus, at high pH the hydrolysis is still acid catalyzed. It follows that activation of the internal aldimine requires not only formation of the ketoamine tautomer but also a net positive charge. The latter is produced in the case of aspartate aminotransferase (16) by protonation of the pyridine ring via an interaction with an aspartate residue as illustrated in

Scheme 4b. In other enzymes that do not have a carboxylate group interacting with the pyridine N, such as alanine racemase and the tryptophan synthase family, the origin of the net positive charge is less clear. If there are no unusual electrostatic interactions, it could be that these enzymes employ a transamination mechanism in which the phenolic oxygen is protonated transiently.

Finally, as mentioned above, although we were not able to detect a geminal diamine of PLP with L-lysine, the study of PLP with diaminopropane shows that under favorable conditions a geminal diamine can be formed. However, it is clear that this process requires deprotonation of the amino group of the incoming amino acid substrate. Whether this process requires also a net positive charge on the aldimine is not clear. Thus, it seems difficult to have the pyridine ring protonated and at the same time the amino group of the substrate deprotonated.

CONCLUSIONS

By measuring the multinuclear NMR spectra of doubly ^{13}C -labeled pyridoxal 5'-phosphate in the presence of ^{15}N -labeled diaminopropane and L-lysine as a function of pH, we have characterized potential reaction partners and intermediates of the transamination reaction (Scheme 1b) of PLP-dependent enzymes. The ^{13}C and ^{15}N chemical shifts of the single-headed Schiff bases formed, as well as of the geminal diamine with diaminopropane, should be useful in future studies of improved model systems. For the first time, the presence of the intramolecular OHN hydrogen bond of PLP Schiff bases has been established by ^{15}N NMR for aqueous solution. In this hydrogen bond, a fast proton tautomerism takes place between a neutral enolimine form and a zwitterionic ketoamine form. The latter is strongly populated even if the pyridine ring is deprotonated. This does not, however, lead to hydrolysis of the Schiff bases, a result which needs to be taken into account in the discussion of the mechanisms of the enzymatic transamination reaction. Furthermore, we have shown that pH controls the occurrence of the different PLP species but that at physiological pH all reactants and potential intermediates except the geminal diamine are present in similar amounts, which is a result of a subtle balance of all functional groups.

SUPPORTING INFORMATION AVAILABLE

The complete sets of NMR spectra depicted partially in Figures 2 and 3, ^{15}N NMR spectra of L-lysine and the corresponding Henderson–Hasselbalch plot, and UV–vis spectra of 1:1 mixtures of pyridoxal 5'-phosphate with diaminopropane plus tables with ^1H , ^{13}C , and ^{15}N NMR chemical shifts and signal intensities. This material is available free of charge via the Internet at <http://pubs.acs.org>.

REFERENCES

1. Metzler, D. E. (1977) *Biochemistry. The chemical reactions of living cells*, Vol. 1, pp 444–461, Academic Press, New York.
2. Snell, E. E., and Jenkins, W. T. (1959) The mechanism of the transamination reaction. *J. Cell. Comp. Physiol.* 54 (Suppl. 1), 161–177.
3. Cordes, E. H., and Jencks, W. P. (1962) Semicarbazone formation from pyridoxal, pyridoxalphosphate, and their Schiff bases. *Biochemistry* 1, 773–778.
4. Tobias, P. S., and Kallen, R. G. (1975) Kinetics and equilibria of the reaction of pyridoxal 5'-phosphate with ethylenediamine to form Schiff-bases, and cyclic geminal diamines. Evidence for kinetically competent geminal diamine intermediates in transamination sequences. *J. Am. Chem. Soc.* 97, 6530–6539.
5. Schirch, L. (1975) Serine transhydroxymethylase-relaxation, and transient kinetic study of formation, and interconversion of enzyme-glycine complexes. *J. Biol. Chem.* 250, 1939–1945.
6. Roy, M., Miles, E. W., Phillips, R. S., and Dunn, M. F. (1988) Detection and identification of transient intermediates in the reactions of tryptophan synthase with oxindolyl-L-alanine and 2,3-dihydro-L-tryptophan. Evidence for a tetrahedral (gem-diamine) intermediate. *J. Biol. Chem.* 27, 8661–8669.
7. Grant, P. L., Basford, J. M., and John, R. A. (1987) An investigation of transient intermediates in the reaction of 2-methylglutamate with glutamate decarboxylase from *Escherichia coli*. *Biochem. J.* 241, 699–704.
8. Ulévitch, R. J., and Kallen, R. G. (1977) Studies of reactions of substituted D,L-erythro-beta-phenylserines with lamb liver serine hydroxymethylase—effects of substituents upon de-aldolization step. *Biochemistry* 16, 5355–5363.
9. Vázquez, M. A., Munoz, F., and Donoso, J. (1992) Transamination reaction between pyridoxal-5'-phosphate Schiff-bases with dodecylamine, and amino-acids. *J. Phys. Org. Chem.* 5, 142–154.
10. Hershey, S. A., and Leussing, D. L. (1977) Rate of carbinolamine formation between pyridoxal 5'-phosphate and alanine. *J. Am. Chem. Soc.* 99, 1992–1993.
11. Christen, P., and Metzler, D. E. (1985) *Transaminases*, 1st ed., pp 37–101, John Wiley & Sons, New York.
12. Snell, E. E., and Di Mari, S. J. (1970) The enzymes—kinetics, and mechanism (Boyer, P. D., Ed.) 3rd ed., Vol. 2, pp 335–362, Academic Press, New York.
13. Sharif, S., Denisov, G. S., Toney, M. D., and Limbach, H. H. (2007) NMR studies of coupled low-, and high-barrier hydrogen bonds in pyridoxal-5'-phosphate model systems in polar solution. *J. Am. Chem. Soc.* 129, 6313–6327.
14. Sharif, S., Schagen, D., Toney, M. D., and Limbach, H. H. (2007) Coupling of functional hydrogen bonds in pyridoxal-5'-phosphate-enzyme model systems observed by solid state NMR spectroscopy. *J. Am. Chem. Soc.* 129, 4440–4455.
15. Sharif, S., Denisov, G. S., Toney, M. D., and Limbach, H. H. (2006) NMR studies of solvent-assisted proton transfer in a biologically relevant Schiff base: towards a distinction of geometric, and equilibrium H-bond isotope effects. *J. Am. Chem. Soc.* 128, 3375–3387.
16. Sharif, S., Fogle, E., Toney, M. D., Denisov, G. S., Shenderovich, I. G., Tolstoy, P. M., Chan-Huot, M., Buntkowsky, G., and Limbach, H. H. (2007) NMR localization of protons in critical enzyme H-bonds. *J. Am. Chem. Soc.* 129, 9558–9559.
17. Sharif, S., Powell, D. R., Schagen, D., Steiner, T., Toney, M. D., Fogle, E., and Limbach, H. H. (2006) X-ray crystallographic structures of enamine, and amine Schiff bases of pyridoxal, and its 1:1 hydrogen bonded complexes with benzoic acid derivatives: evidence for coupled inter- and intramolecular proton transfer. *Acta Crystallogr. B* 62, 480–487.
18. Sharif, S., Chan-Huot, M., Tolstoy, P. M., Toney, M. D., Jonsson, K. H. M., and Limbach, H. H. (2007) ^{15}N NMR studies of acid-base properties of pyridoxal 5'-phosphate aldimines in aqueous solution. *J. Phys. Chem. B* 111, 3869–3876.
19. Shaw, J. P., Petsko, G. A., and Ringe, D. (1997) Determination of the structure of alanine racemase from *Bacillus stearothermophilus* at 1.9-Å Resolution. *Biochemistry* 36, 1329–1342.
20. Major, D. T., and Gao, J. (2006) A combined quantum mechanical and molecular mechanical study of the reaction mechanism and α -amino acidity in alanine racemase. *J. Am. Chem. Soc.* 128, 16345–16357.
21. Cook, P. D., and Holden, H. M. (2007) A structural study of GDP-4-keto-6-deoxy-D-mannose-3-dehydratase: caught in the act of geminal diamine formation. *Biochemistry* 46, 14215–14224.
22. Peterson, E. A., and Sober, H. A. (1954) Preparation of crystalline phosphorylated derivatives of vitamin B₆. *J. Am. Chem. Soc.* 76, 169–175.
23. Jo, B. H., Nair, V., and Davis, L. (1977) Carbon-13 nuclear magnetic resonance studies of vitamin B₆ Schiff base and carbinolamine formation in aqueous solution. 1. The adduct of pyridoxal 5'-phosphate, and DL-alanine. *J. Am. Chem. Soc.* 99, 4467–4471.
24. Donoso, S. A., Frau, J., and Munoz, F. (2004) Density functional theory studies on transamination of vitamin B₆ analogues through geminal diamine formation. *J. Phys. Chem. A* 108, 11709–11714.
25. Metzler, C. M., Cahill, A., and Metzler, D. E. (1980) Equilibria and absorption spectra of Schiff bases. *J. Am. Chem. Soc.* 102, 6075–6082.
26. Christensen, H. N. (1958) Three Schiff base types formed by amino acids, peptides and proteins with pyridoxal and pyridoxal 5'-phosphate. *J. Am. Chem. Soc.* 80, 99–105.
27. Metzler, D. E. (1957) Equilibria between pyridoxal and amino acids and their imines. *J. Am. Chem. Soc.* 79, 485–490.
28. Robitaille, P. M., Scott, R. D., Wang, J., and Metzler, D. E. (1989) Schiff bases and geminal diamines derived from pyridoxal 5'-phosphate and diamines. *J. Am. Chem. Soc.* 111, 3034–3040.
29. Haran, R., Laurent, J. P., Massol, M., and Nepveu-Juras, F. (1980) Vitamin B₆, and derivatives. II— ^{13}C NMR study of systems formed

- by pyridoxal phosphate, and pyridoxal with octopamine. *Org. Magn. Res.* 14, 45–48.
30. Tsai, M. D., Byrn, S. R., Chang, C., Floss, H. G., and Weintraub, H. J. R. (1978) Conformational analysis of pyridoxal Schiff's bases. Nuclear magnetic resonance studies of the conformations about the C₄-C_{4'}, C_α-C_β, and N-C_α bonds of the pyridoxal Schiff's bases of amino acids. *Biochemistry* 17, 3177–3182.
31. Chan-Huot, M., Niether, C., Sharif, S., Tolstoy, P. M., Toney, M. D., and Limbach, H. H. (2010) NMR Studies of the protonation states of pyridoxal 5'-phosphate in water. *J. Mol. Struct.* 976, 282–289.
32. Kenniston, R. C. (1979) Polyamine-pyridoxal 5'-phosphate interaction: effects of pH, and phosphate concentration in Schiff's base formation. *Physiol. Chem. Phys.* 11, 465–470.
33. O'Leary, M., and Payne, J. R. (1976) ¹³C NMR spectroscopy of labeled pyridoxal 5'-phosphate. *J. Biol. Chem.* 251, 2248–2254.
34. Scherer, G., and Limbach, H.-H. (1994) Dynamic NMR study of the tautomerism of bicyclic oxalamidines: kinetic HH/HD/DD isotope and solvent effects. *J. Am. Chem. Soc.* 116, 1230–1239.
35. Finseth, F., and Sizer, I. W. (1967) Complexes of pyridoxal phosphate with amino acids, peptides, polylysine, and apotransaminase. *Biochem. Biophys. Res. Commun.* 26, 625–630.
36. Huang, T.-C., Chen, M.-H., and Ho, C.-T. (2001) Effect of phosphate on stability of pyridoxal in the presence of lysine. *J. Agric. Food Chem.* 49, 1559–1563.
37. Bongini, A., and Arcelli, A. (1980) ¹H NMR study of the reaction of ornithine, and lysine with pyridoxal 5'-phosphate. *Org. Magn. Res.* 13, 328–329.
38. Dawson, R. M. C., Elliot, W. H., and Jones, K. M. (1986) Data for biochemical research, 3rd ed., Clarendon Press, Oxford.
39. Naulet, N., Tomé, D., and Martin, G. J. (1983) ¹⁵N nuclear magnetic resonance studies of amino acids, and their reaction products with formaldehyde. *Org. Magn. Res.* 21, 564–566.
40. Hayashi, S., and Hayamizu, K. (1991) Chemical shift standards in high resolution solid state NMR (2) ¹⁵N nuclei. *Bull. Chem. Soc. Jpn.* 64, 688–690.
41. Po, H. N., and Senozan, N. M. (2001) The Henderson–Hasselbalch equation: its history, and limitations. *J. Chem. Educ.* 78, 1499–1503.
42. De Levie, R. (2003) The Henderson–Hasselbalch equation: its history, and limitations. *J. Chem. Educ.* 80, 146.
43. Blomberg, F., Maurer, W., and Rüterjans, H. (1977) Nuclear magnetic resonance investigation of ¹⁵N-labeled histidine in aqueous solution. *J. Am. Chem. Soc.* 99, 8149–8159.
44. Golubev, N. S., Smirnov, S. N., Tolstoy, P. M., Sharif, S., Toney, M. D., Denisov, G. S., and Limbach, H. H. (2007) Observation by NMR of the tautomerism of an intramolecular OHOHN-charge relay chain in a model Schiff base. *J. Mol. Struct.* 844, 319–327.
45. Toney, M. D., and Kirsch, J. F. (1993) Lysine 258 in aspartate aminotransferase: enforcer of the circe effect for amino acid substrates and general-base catalyst for the 1,3-prototropic shift. *Biochemistry* 32, 1471–1479.